

Cation- and vacancy-ordering in Li_xCoO_2

C. Wolverton and Alex Zunger
 National Renewable Energy Laboratory, Golden, CO 80401
 (August 27, 2018)

Using a combination of first-principles total energies, a cluster expansion technique, and Monte Carlo simulations, we have studied the Li/Co ordering in LiCoO_2 and Li-vacancy/Co ordering in the $\square\text{CoO}_2$. We find: (i) A ground state search of the space of substitutional cation configurations yields the CuPt structure as the lowest-energy state in the octahedral system LiCoO_2 (and $\square\text{CoO}_2$), in agreement with the experimentally observed phase. (ii) Finite temperature calculations predict that the solid-state order-disorder transitions for LiCoO_2 and $\square\text{CoO}_2$ occur at temperatures (~ 5100 K and ~ 4400 K, respectively) much higher than melting, thus making these transitions experimentally inaccessible. (iii) The energy of the reaction $E_{\text{tot}}(\sigma, \text{LiCoO}_2) - E_{\text{tot}}(\sigma, \square\text{CoO}_2) - E_{\text{tot}}(\text{Li}, \text{bcc})$ gives the average battery voltage \bar{V} of a $\text{Li}_x\text{CoO}_2/\text{Li}$ cell for the cathode in the structure σ . Searching the space of configurations σ for large average voltages, we find that $\sigma=\text{CuPt}$ (a monolayer (111) superlattice) has a high voltage ($\bar{V}=3.78$ V), but that this could be increased by cation randomization ($\bar{V}=3.99$ V), partial disordering ($\bar{V}=3.86$ V), or by forming a 2-layer $\text{Li}_2\text{Co}_2\text{O}_4$ superlattice along (111) ($\bar{V}=4.90$ V).

I. INTRODUCTION

Much like the ABC_2 semiconductors ($A, B = \text{Al, Ga, In}$ and $C = \text{N, P, As, or Sb}$) exhibit cation ordering in a tetrahedrally-coordinated network¹, the LiMO_2 oxides ($M=3d$ transition metal)^{2,3} form a similar series of structures based on the octahedrally-coordinated network with anions (O) on one fcc sublattice and cations (Li and M) on the other (Fig. 1). Cation arrangements in isovalent (III-III-V) or heterovalent (I-III-VI) semiconductor alloys have been observed¹ in the disordered, CuAu-type (CA), CuPt-type (CP), and chalcopyrite (CH) structures (bottom row of Fig. 1), while cation arrangements in the oxides have been observed^{2,3} in the disordered, CP, CH, D4, and Y2 structures (top row of Fig. 1). *Ab-initio* total energy calculations¹ have shown that in the tetrahedrally-coordinated III-V semiconductor alloys, the CuPt structure is the least stable [due to the fact that it represents a stacking along the elastically hard (111) direction], while the chalcopyrite structure is most stable (it possesses both the lowest electrostatic and strain energies). Similar studies have been performed for the octahedrally-coordinated networks of the spin alloy $\text{Mn}^\uparrow\text{S}-\text{Mn}^\downarrow\text{S}$ and the lead chalcogenides.⁴ In this paper, we examine the energetics and thermodynamics of cation ordering tendencies in the octahedral LiCoO_2 oxide, and compare to the tetrahedral semiconductor case which is well studied. The LiCoO_2 compound is used as a cathode material in rechargeable Li batteries.^{5,6,7,8,9,10,11,12,13,14} When Li is de-intercalated from the compound, it creates a vacancy (denoted \square) that can be positioned in different lattice locations. Hence, we will examine not only (a) the Li/Co cation ordering (different sites for Li and Co) prop-

erties of LiCoO_2 ($x_{\text{Li}}=1$), but also (b) the vacancy/Co ordering (different sites for \square and Co) in $\square\text{CoO}_2$ ($x_{\text{Li}}=0$). A third type of ordering in these materials, vacancy/Li ordering in $\text{Li}_x\square_{1-x}\text{CoO}_2$ ($0 \leq x_{\text{Li}} \leq 1$), is not treated here.

Our calculation proceeds in three steps: (1) *Total energy calculations*: We calculate the $T=0$ total energy of a set of (not necessarily stable) ordered structures via the full potential, all-electron linearized augmented plane wave method (LAPW)^{15,16} with all atomic positions fully relaxed via quantum mechanical forces. We then map those energies onto a (2) *cluster expansion (CE)*.^{17,18,19,20,21,22} This expansion is a generalized Ising-like expression for the energy of an *arbitrary* substitutional cation arrangement. Once the coefficients of the expansion are known, the Ising-like expression may be easily evaluated for any cation configuration. Thus, one can calculate (via first-principles) the total energy of a *few* cation arrangements, but then effectively search the space of 2^N configurations (where N is typically $\lesssim 10^4$). Specifically, the cluster expansion may be used to search the entire configurational space for stable ground state structures, where one can obtain low energy, but otherwise unsuspected states (i.e., states which are not included in the set of calculated total energies). Having obtained such a general and computationally simple parameterization of the configuration energy, we subject it to (3) *Monte Carlo simulated annealing*²³ to extend first-principles calculations (at zero temperature) to finite-temperatures, thus obtaining order-disorder transition temperatures and thermodynamic functions.

We find for LiCoO_2 the following:

- (a) A ground state search of the space of substitutional

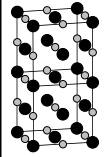
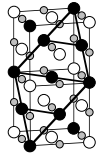
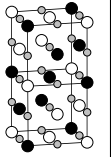
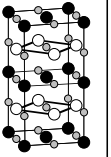
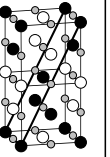
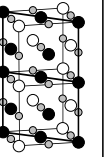
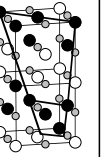
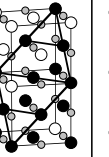
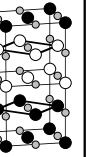
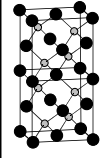
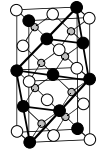
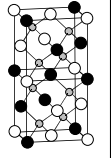
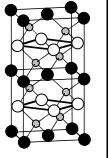
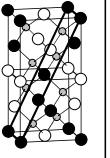
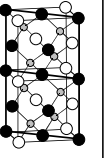
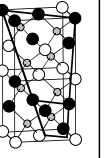
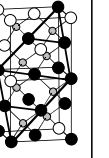
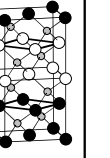
	Disordered	CuPt-type (CP)	D4	CuAu-type (CA)	Chalcopyrite (CH)	Y2	W2	V2	Z2
Octahedral (Rocksalt)									
Tetrahedral (Zincblende)									
Cation Superlattice	---	(1,1) along [111]	---	(1,1) along [001]	(2,2) along [201]	(2,2) along [110]	(2,2) along [311]	(2,2) along [111]	(2,2) along [100]

FIG. 1. Cation arrangements in tetrahedral (semiconductor) and octahedral (oxide) networks. The black and white atoms represent the cations, while the grey atoms are the anions. Shown are the names of the cation configurations, the structure itself (bold lines indicate superlattice planes), and the equivalent superlattice of cations. Note: Some of the structures are shown as only a portion of the complete unit cell.

cation configurations yields the CuPt structure as the ground state in the octahedral LiCoO_2 system, in agreement with the well-established experimentally observed phase.⁵ We find that this result holds even if the CuPt structure is not included in the set of energies used to fit the CE parameterization. The CuPt cation structure is the least stable bulk structure in tetrahedral ABC_2 .

(b) Finite temperature calculations predict that the solid-state order-disorder transition for LiCoO_2 occurs at temperatures (~ 5100 K) much higher than melting, thus making this transition experimentally inaccessible. In contrast, order-disorder transitions in isovalent tetrahedral ABC_2 systems are $\lesssim 1000$ K.¹ The addition of Li vacancies lowers this transition to ~ 4400 K; but, this transition temperature is still too high to be observed. Thus, the finite temperature calculations demonstrate that the observed disordered (rocksalt) phase of LiCoO_2 is not thermodynamically stable, but is only stabilized kinetically.

(c) The energy of intercalation reaction $E_{\text{tot}}(\sigma, \text{LiCoO}_2) - E_{\text{tot}}(\sigma, \square\text{CoO}_2) - E_{\text{tot}}(\text{Li}, \text{bcc})$ gives the average battery voltage \bar{V} of a $\text{Li}_x\text{CoO}_2/\text{Li}$ cell for the cathode in the structure σ ,⁶ thus providing a means for prediction of battery intercalation voltages from first-principles energetics. Searching the space of configurations σ for large average voltages, we find that $\sigma = \text{CuPt}$ [a monolayer (111) superlattice] has a high voltage ($\bar{V} = 3.78$ V), but that this could be increased by cation randomization ($\bar{V} = 3.99$ V), partial disordering ($\bar{V} = 3.86$ V), or by forming a 2-layer $\text{Li}_2\text{Co}_2\text{O}_4$ superlattice along $\langle 111 \rangle$ ($\bar{V} = 4.90$ V).

(d) Ordered cation arrangements in LiCoO_2 are *sta-*

ble, similar to the heterovalent tetrahedral I-III-VI₂ (e.g., CuInSe_2) systems²⁴, but is the opposite situation from the isovalent tetrahedral III-V systems such as GaInP_2 , in which bulk ordered compounds are *unstable*.

(e) The relative order of structural energies in the octahedral LiCoO_2 system is quite different from the tetrahedral cases: $E(\text{CuPt}) < E(\text{CH}) < E(\text{CA})$ in both LiCoO_2 and $\square\text{CoO}_2$, compared with $E(\text{CH}) < E(\text{CA}) < E(\text{CuPt})$, universally found in the lattice-mismatched tetrahedral systems (Fig. 2).

II. METHODS OF CALCULATION

We use the cluster expansion (CE) technique,^{17,19,20,21,22} which consists of an Ising-like expression in which each cation is associated with the site of an ideal lattice (fcc, in this case), and the pseudo-spin variable S_i is given the value $+1(-1)$ if an $A(B)$ atom is assigned to site i . Within this description, the energy of *any* configuration σ of cations can be written as:¹⁹

$$E_{\text{CE}}(\sigma) = \sum_f D_f J_f \bar{\Pi}_f(\sigma), \quad (1)$$

where f is a figure comprised of several lattice sites (pairs, triplets, etc.), D_f is the number of figures per lattice site, J_f is the Ising-like interaction for the figure f , and $\bar{\Pi}_f$ is a function defined as a product over the figure f of the variables S_i , averaged over all symmetry equivalent figures of lattice sites. This expression incorporates the

TABLE I. Lattice averaged spin products $\overline{\Pi}_f(\sigma)$ (for a few figures f) of the cation configurations σ shown in Fig. 1.

Interaction	Figure f	D_f	$\overline{\Pi}_f(\sigma)$									
			AC+BC	CP	D4	Y2	CH	CA	W2	V2	Z2	Random $x=1/2$
J_0	Empty	1	1	1	1	1	1	1	1	1	1	1
J_1	Point	0	0	0	0	0	0	0	0	0	0	0
J_2	NN Pair	6	1	0	0	0	-1/3	-1/3	-1/6	1/2	1/3	0
K_2	2NN Pair	3	1	-1	-1	-1/3	1/3	1	0	0	1/3	0
L_2	3NN Pair	12	1	0	0	0	1/3	-1/3	0	0	-1/3	0
M_2	4NN Pair	6	1	1	1	-1/3	-1/3	1	0	0	-1/3	0
N_2	5NN Pair	12	1	0	0	0	-1/3	-1/3	1/6	-1/2	1/3	0
O_2	6NN Pair	4	1	-1	-1	1	-1	1	0	0	-1	0
P_2	7NN Pair	24	1	0	0	0	1/3	-1/3	0	0	-1/3	0
Q_2	8NN Pair	3	1	1	1	1	1	1	-1	-1	1	0
R_2	9NN Pair	6	1	0	0	0	-1/3	-1/3	-1/6	1/2	1/3	0
S_2	10NN Pair	12	1	0	0	0	-1/3	-1/3	1/6	-1/2	1/3	0
J_4	Tetrahedron	2	1	-1	1	-1	1	1	0	0	1/3	0

effects of atomic relaxation (indeed, one does not require that the cations sit precisely at the ideal lattice positions, but merely that there is a one-to-one correspondence between lattice sites and atomic positions).²⁵ We determine $\{J_f\}$ by fitting $E_{CE}(\sigma)$ of N_σ structures to LDA total energies $E_{LDA}(\sigma)$, given the matrices $\{\overline{\Pi}_f(\sigma)\}$ for these structures. Table I gives the values of the lattice-averaged spin products $\overline{\Pi}_f(\sigma)$ and degeneracies D_f for the structures in Fig. 1. The values of $\overline{\Pi}_f(\sigma)$ sometimes take on interesting degeneracies: For example, CA and CH differ only by $\overline{\Pi}_f(\sigma)$ for figures beyond the nearest neighbor, and the CuPt and D4 structures have^{3,26} equivalent pair correlation functions for *all* pair separations. Also, all odd-body correlation functions are zero for any structure which possesses $A \rightarrow B$ (or $\hat{S}_i \rightarrow -\hat{S}_i$) symmetry, such as all those shown in Fig. 1. This means that CuPt and D4 possess not only equivalent pair correlations, but three-body correlations as well. Thus, in terms of Eq. (1), all terms in the expansion which correspond to one-, two-, and three-body figures do not distinguish between CuPt and D4, and thus the first cluster correlation which can break the degeneracy between these two structures is in the four-body terms. In spite of the similarities between the CuPt and D4 structures, the former is a superlattice along the [111] direction and hence is rhombohedral, while the latter is not a superlattice and is cubic (see Fig. 1). Thus, the CuPt structure has one extra structural degree of freedom (namely a c/a ratio) that the D4 structure does not have.²⁷

We use $N_\sigma = 8$ configurations in the fitting procedure. These are shown in Fig. 1. The choice of end-point configurations requires some discussion. The nominal end point configurations, LiO and CoO in the NaCl structure, do not obey the octet rule, as LiO has 7 valence electrons/formula unit, while CoO has (in addition to its filled t_{2g} shell) 9 valence electrons/formula. As a result, these nominal structures have a very high energy. In the 1:1 structures $(\text{LiO})_n(\text{CoO})_n$, an electron

will move from each CoO unit to fill the hole in the LiO unit, thus creating normal octet bonds. These “charge compensated” end-point compounds $(\text{LiO})^*$ and $(\text{CoO})^*$ will have a lower energy than the nominal LiO and CoO. Our calculations thus consider only charge compensated structures. Using the procedure of Wei *et al.*²⁴ in treating heterovalent alloys, the conventional, high-energy “end-point” compounds LiO+CoO are not included in the CE because they are not charge compensated. Our CE could be used to *predict* the energies of $(\text{LiO})^* + (\text{CoO})^*$, and we will see that this energy is indeed lower than that of nominal LiO+CoO. We only include the eight $(\text{LiO})_n(\text{CoO})_n$ compounds shown in Fig. 1 in our fit. These cation orderings correspond to both the observed structures in the LiMO_2 series (CuPt, D4, Y2, and CH) as well as other cation arrangements not observed in this series (CuAu, W2, V2, and Z2). For substitutional ordering problems, it is possible to enumerate all configurations up to a given unit cell size.²⁸ The set of cation configurations considered here includes all of the possible equiatomic structures with unit cell size up to eight atoms.

The set of twelve figures f retained in the expansion is the “empty” figure, the first ten neighbor pairs, and the nearest neighbor tetrahedron. In fitting the LDA total energies to the cluster expansion, we include a Lagrange multiplier with the constraint that the pair interactions should be as smooth as possible in reciprocal space. This technique (more fully explained in Ref. 29) allows one to retain more figures in the expansion than total energies, and also requires the pair interactions to be as convergent as possible in real space. Although more sophisticated versions of the cluster expansion approach²⁹ are available when one requires extreme accuracy and has access to a large database of structural energies, we use the simple real-space expansion of Eq. (1) with the Lagrange multiplier. The use of this simple form is predicated on the assumption that if we specialize

TABLE II. Predicted structural information of observed LiCoO₂ phases. Where available, experimental data and other calculated results are shown. CuPt - ABC and CuPt - AAA refer to CuPt configurations of cations (alternately stacked Li/Co or □/Co close-packed layers) in ABC... or AAA... type stackings, respectively. For □CoO₂, CuPt - ABC and CuPt - AAA are isostructural with CdCl₂ and CdI₂, respectively. Bulk moduli for LiCoO₂ (CuPt) and □CoO₂ (CuPt) were calculated (present work) to be 2.4 and 2.8 Mbar, respectively.

Compound	Method	a (Å)	c (Å)	Li-O (Å)	Co-O (Å)	V_{eq} (Å ³)
LiCoO ₂ (CuPt - ABC)	Expt. ^a	2.82	14.04	2.07	1.94	32.23
	FLAPW (present work)	2.81	13.60	2.08	1.90	31.2
	Pseudopot. ^b	2.93	13.2	2.10	1.96	32.71
□CoO ₂ (CuPt - ABC)	FLAPW (present work)	2.78	12.13		1.85	26.9
	Pseudopot. ^b	2.88	12.26		1.90	29.36
LiCoO ₂ (CuPt - AAA)	FLAPW (present work)	2.79	4.74	2.11	1.90	32.0
□CoO ₂ (CuPt - AAA)	Expt. ^c	2.822	4.29		1.91	29.6
	FLAPW (present work)	2.80	4.01		1.85	27.1
LiCoO ₂ (D4)	Expt. ^d	8.002		2.06	1.95	32.0
	FLAPW (present work)	7.90		2.05	1.91	30.7
□CoO ₂ (D4)	FLAPW (present work)	3.85			1.85	28.5

^aRef. 13

^bRef. 36

^cRef. 11

^dRef. 40

to fixed composition (e.g., either $x_{\text{Li}}=1$ or $x_{\text{Li}}=0$) the expansion converges quickly with a small number of terms. For our CE, the error in the input energies used in the fit is a negligible amount, < 1 meV/formula unit. To obtain some idea of the errors involved in the CE predictions, we have removed some structures and figures from the fitting process, and examined the resulting errors: Removing the CuPt (CH) structure and the four-body tetrahedron figure from the fit produces an 11 (49) meV/formula unit error in the energy of CuPt (CH), negligible changes in the other fitted energies, and an energy of the random cation arrangement which changes by only 1 (7) meV/formula unit. The magnitude of these errors is quite small in terms of the energetic scales of cation ordering (~ 1000 - 2000 meV/formula unit) and Li intercalation (~ 4000 meV/formula unit).

The expression of Eq. (1) can be applied to different ordering problems, with a separate expansion constructed for each situation. Here, we construct three separate cluster expansions to describe three different types of structural energetics:

(a) Formation enthalpies for different Li/Co arrangements σ on the fcc lattice:

$$\Delta H_f(\sigma, \text{LiCoO}_2) = E_{\text{tot}}(\sigma, \text{LiCoO}_2) - E_{\text{tot}}(\text{LiO}, B1) - E_{\text{tot}}(\text{CoO}, B1) \quad (2)$$

where the last two terms refer to LiO and CoO in the NaCl (B1) structure with lattice constants obtained by minimizing the respective total energies with respect to

hydrostatic deformation. The resulting CE will reveal Li/Co ordering tendencies at $x_{\text{Li}}=1$.

(b) Formation enthalpies for different □/Co arrangements σ on the fcc lattice:

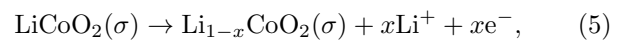
$$\Delta H_f(\sigma, \square\text{CoO}_2) = E_{\text{tot}}(\sigma, \square\text{CoO}_2) + E_{\text{tot}}(\text{Li}, \text{bcc}) - E_{\text{tot}}(\text{LiO}, B1) - E_{\text{tot}}(\text{CoO}, B1) \quad (3)$$

where $E_{\text{tot}}(\text{Li}, \text{bcc})$ is the total energy of Li in the bcc structure with lattice constant obtained from total energy minimization. The resulting CE will reveal □/Co ordering tendencies at $x_{\text{Li}}=0$.

(c) The Li battery intercalation reaction energy for different Li/Co (and □/Co) arrangements on the fcc lattice:

$$\Delta H_{\text{react}}(\sigma) = E_{\text{tot}}(\sigma, \text{LiCoO}_2) - E_{\text{tot}}(\sigma, \square\text{CoO}_2) - E_{\text{tot}}(\text{Li}, \text{bcc}) \quad (4)$$

ΔH_{react} is the energy gained upon complete deintercalation of Li from LiCoO₂, relative to Li metal, and is simply the difference between Eq. (2) and Eq. (3). If one assumes that the Li is removed without a change of the cathode structure σ (a topotactic reaction),



then (see, e.g., Ref. 6) the reaction energy ΔH_{react} of Eq. (4) is equal to the integral of the (zero temperature and pressure) open circuit voltage V of a Li _{x} CoO₂/Li cell between Li compositions $x_{\text{Li}}=0$ and $x_{\text{Li}}=1$:

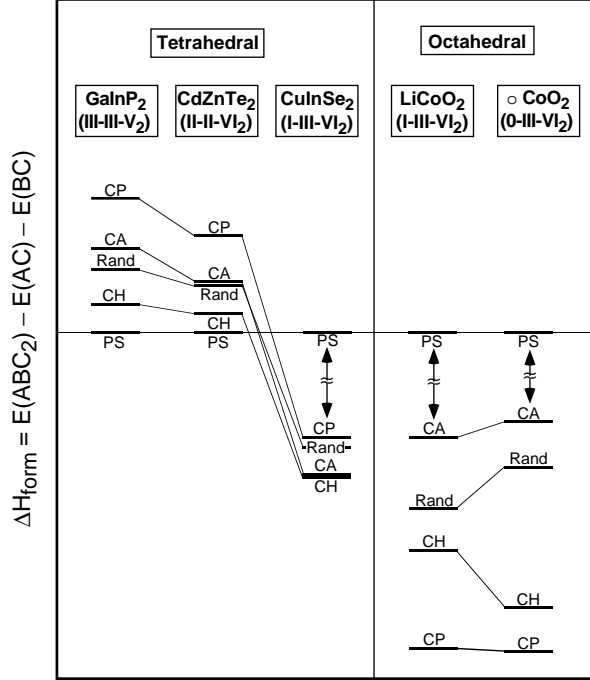


FIG. 2. Formation energies of cation ordering in tetrahedral and octahedral ABC_2 compounds in structures shown in Fig. 1. For the $GaInP_2$ and $CdZnTe_2$ compounds, the energy scale was multiplied by 5 for visual clarity. The $GaInP_2$, $CdZnTe_2$, and $CuInSe_2$ energetics were taken from Refs. 38, 39, 24, respectively. The $LiCoO_2$ and $\square CoO_2$ energetics are from the present work. “PS” represents the energy of a phase-separated mixture of AC+BC rocksalt (zincblende) binaries in the octahedral (tetrahedral) systems. “Rand” is the energy of a phase in which cations are distributed randomly (i.e., with no correlations) on their sublattice.

$$\Delta H_{\text{react}}(\sigma) = -F \int_0^1 dx V(\sigma, x) = -\bar{V}(\sigma) \quad (6)$$

where F is the Faraday constant. Hence, $|\Delta H_{\text{react}}|$ is simply the intercalation voltage *averaged* over Li composition. We note that the intercalation voltage calculated in this manner is a bulk, thermodynamic quantity and does not contain contributions from the cathode surface or from kinetic phenomena.

The total energies needed for Eqs. (2)-(4) have been obtained using the first-principles full-potential LAPW¹⁵ method. In the LAPW calculations, we used the exchange correlation of Ceperley and Alder as parameterized by Perdew and Zunger.³⁰ LAPW sphere radii were chosen to be 2.0, 2.0, and 1.3 a.u. for Li, Co, and O, respectively. A well converged basis set was used, corresponding to an energy cutoff of 25.5 Ry ($RK_{\text{max}}=6.57$). Tests were performed placing the Co $3p$ levels in a sepa-

rate semi-core energy window as opposed to treating the Co $3p$ as a core state; negligible differences were found, and thus the latter was used in all the calculations described below. Brillouin-zone integrations are performed using the equivalent \mathbf{k} -point sampling method, using \mathbf{k} -points for each structure corresponding to the same 28 (6x6x6) special \mathbf{k} -points for the fcc structure.³¹ All total energies are optimized with respect to volume as well as all cell-internal and -external coordinates. Convergence tests of the energy differences (with respect to basis function cutoff, \mathbf{k} -point sampling, and muffin-tin radii) indicate that the total energy differences are converged to within ~ 0.01 - 0.02 eV/formula unit.

Spin polarized calculations were performed for $LiCoO_2$ and $\square CoO_2$ in the CuPt cation arrangement in both ferromagnetic (FM) and anti-ferromagnetic (AFM) geometries. For $LiCoO_2$, both the FM and AFM calculations converged to the non-magnetic solution ($\mu_{Co}=0$). However, for $\square CoO_2$, both FM and AFM calculations showed a weakly magnetic solution ($\mu_{Co} \sim 0.45$ for both FM and AFM) with the total energy of the FM (AFM) state being 14 (~ 0) meV/formula unit below the non-magnetic state. Because spin polarization only has a small effect on the energy of these compounds, the calculations below for the energetics of cation ordering in $LiCoO_2$ and $\square CoO_2$ are non-magnetic (NM). NM, FM, and AFM (with the observed alternating [111] layers of spins) calculations were also performed for CoO, with the AFM solution being lowest in energy, and hence used here.³²

Having obtained the coefficients $\{J_f\}$ of the CE for Eq. (1) for the three types (a)-(c) of ordering reactions, we subjected $E_{CE}(\sigma)$ to a Monte Carlo simulated annealing method for treating the configurational thermodynamics.²³ A system size of $16^3 = 4096$ atoms (with periodic boundary conditions) was used in all calculations. Monte Carlo simulations were performed in the canonical ensemble with the transition temperatures being calculated from the discontinuity in the internal energy as a function of temperature, and the ground states determined from the simulation at a temperature where all configurational changes proved to be energetically unfavorable. This gives: (i) the $T=0$ K ground state structures (from a simulation of a finite size cell initially at high temperature, and subsequently slowly cooled to a low temperature where all configurational changes proved to be energetically unfavorable), (ii) the pair correlation functions or atomic short-range order present in the disordered alloy, and (iii) the order-disorder transition temperature, T_c .

III. $T = 0$ FORMATION ENERGIES

A. Energetics of Li/Co ordering in $LiCoO_2$

The formation energies [Eq. (2)] of $LiCoO_2$ in various cation arrangements are given in Table III and calculated

TABLE III. FLAPW calculated formation energies (eV/formula unit) of various cation arrangements in LiCoO₂ and □CoO₂+Li(bcc): $\Delta H_f(\sigma, \text{LiCoO}_2)$, $\Delta H_f(\sigma, \square\text{CoO}_2)$, (formation energies of σ) and $\Delta H_{\text{react}}(\sigma)$ (average intercalation voltage of LiCoO₂ relative to Li) are defined in Eqs. (2)-(4). V_{eq} is the equilibrium volume (\AA^3 /formula unit) of LiCoO₂, and δV is the change in volume upon Li extraction [i.e., $V_{\text{eq}}(\text{LiCoO}_2) - V_{\text{eq}}(\square\text{CoO}_2)$]. All energies of various ordered, disordered, and partially-ordered cation arrangements in LiCoO₂ are from cluster expansions (CE) of FLAPW energetics, and are described in the text.

Cation Structure	LiCoO ₂	□CoO ₂ +Li(bcc)	ΔH_{react}	V_{eq}	δV
	$\Delta H_f(\sigma)$	$\Delta H_f(\sigma)$			
CuPt	-3.38	+0.40	-3.78	31.3	4.3
D4	-3.37	+0.54	-3.91	30.5	1.9
Y2	-3.07	+0.80	-3.87	31.4	1.9
CH	-2.84	+0.64	-3.48	30.8	3.2
W2	-2.82	+0.94	-3.76	30.6	3.1
CuAu	-2.23	+1.65	-3.88	29.5	3.8
V2	-2.02	+2.88	-4.90	31.3	1.0
Z2	-2.13	+2.38	-4.51	31.5	2.2
Random($\eta=0, \text{SRO}=0$)	-2.68	+1.31	-3.99		
Disordered($\eta=0, \text{SRO}\neq 0$)	-2.95	+0.91	-3.86		
CuPt($\eta=0.88, \text{SRO}=0$)	-3.22	+0.60	-3.82		
D4($\eta=0.88, \text{SRO}=0$)	-3.21	+0.71	-3.92		

structural properties are shown in Table II. We note that the D4 structure is only slightly higher in energy than the CuPt structure. This competition is interesting because LiCoO₂ has been synthesized in the D4 structure by solution growth at low temperature.^{3,7,8,9,10,33,34,35} (Although there was initially some discussion in the literature about this low-temperature synthesized phase being CuPt with imperfect long-range order⁷, it is now established that this phase is D4 (or “D4-like”).^{3,33,9,10,34}) The near degeneracy of the calculated energies of the CuPt and D4 structures is simply a consequence of their identical pair and three body correlations $\bar{\Pi}_f(\sigma)$ noted above. We will see that the four-body interaction J_4 which distinguishes these structures is quite small, consistent with the small energy difference between CuPt and D4.

B. Energetics of □/Co ordering in □CoO₂

The formation energies [Eq. (3)] of □CoO₂ in various □/Co arrangements are also given in Table III. These configurations correspond to various arrangements of Co and □. We note the following:

(1) The relative order of energetics is similar in □CoO₂ as in LiCoO₂. There is only one qualitative difference: CH drops in energy significantly upon extraction of Li, and is lower in energy than the Y2 structure, whereas the reverse is true for LiCoO₂.

(2) The separation in energy between CuPt and D4 increases in □CoO₂ compared to LiCoO₂, due to the symmetry of the phases: Upon extraction of Li in the rhombohedral CuPt structure, the c/a ratio decreases significantly, providing a significant source of energy lowering for □CoO₂ - CuPt. D4, on the other hand, is not a layered superlattice in any direction and has cubic symmetry. Hence, the cell parameters of □CoO₂ (D4) can-

not distort in any preferred direction, and consequently, □CoO₂ (D4) does not relax as much as CuPt.

(3) The CuPt structure of □CoO₂ (isostructural with CdCl₂) has an ABC... stacking of the cation planes. However, recent electrochemical measurements of Amatucci *et al.*¹¹ have succeeded in completely deintercalating Li from LiCoO₂, forming a □CoO₂ structure which is isostructural with CdI₂, with the stacking of planes in an AAA... arrangement (see Fig. 3) which we call “CuPt (AAA)”. These two structure are not related to one another by substitutional degrees of freedom, and thus are not describable by a single cluster expansion. To examine these non-substitutional degree of freedom, we have performed total energy calculations of □CoO₂ in both the CuPt and CuPt (AAA) structures (CdI₂). Consistent with the observations of Amatucci *et al.*¹¹, we find that the □CoO₂ in the AAA stacking is lower in energy than the CuPt structure by ~ 0.05 eV/formula unit.

(4) We find that LiCoO₂ in the CuPt (AAA) structure (Fig. 3) is higher in energy than the CuPt structure (with ABC stacking) by ~ 0.15 eV/formula unit, in agreement with the fact that the observed CuPt ground state in LiCoO₂ has ABC stacking.

C. Effect of cation arrangement on average voltages

Table III gives the calculated reaction energies given in Eq. (4) for each of the cation arrangements σ studied here. The average voltages for all cation arrangements considered are in the ~ 4 V range. In particular, the average voltage for LiCoO₂ in the CuPt structure (3.78 V) is in reasonable agreement with measured values (4.0-4.2 V)^{5,12,13,11} and pseudopotential calculations (3.75 V).³⁶ Some configurations like CH, show a marked relaxation

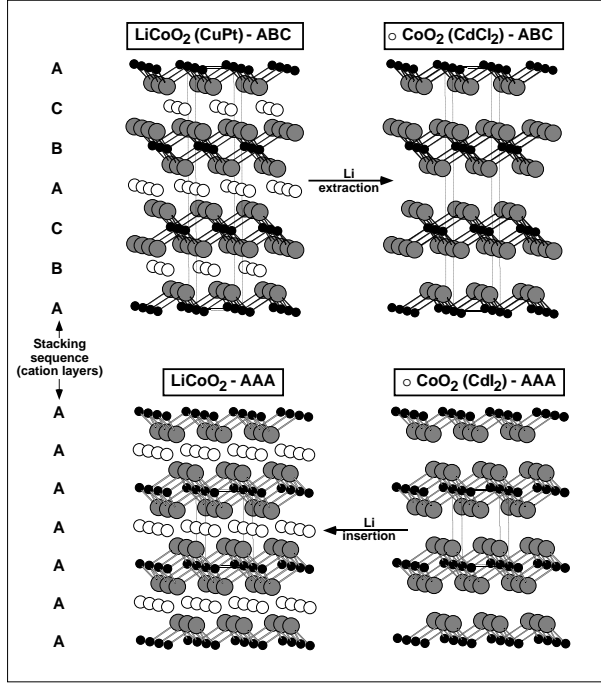


FIG. 3. Different stacking arrangements of close packed cation planes in LiCoO_2 and $\square\text{CoO}_2$. The white, black and grey atoms represent Li, Co, and O, respectively. Clockwise from the top left, the structures are: (i) The stable LiCoO_2 (CuPt) phase (equivalent to the phase shown in Fig. 1 but from a point of view which emphasizes the layered nature of the compound) with close packed cation planes in the ABC... fcc stacking. (ii) The $\square\text{CoO}_2$ (CuPt) structure (isostructural with CdCl_2) formed from extracting Li from the LiCoO_2 structure, with close packed cation planes in an ABC... stacking. (iii) The observed $\square\text{CoO}_2$ phase “CuPt (AAA)” (isostructural with CdI_2) which corresponds to an AAA... stacking of close packed cation planes. (iv) A hypothetical LiCoO_2 structure “CuPt (AAA)”, formed from insertion of Li into the $\square\text{CoO}_2$ (CdI_2) phase.

of the $\square\text{CoO}_2$ phase, and hence show a significantly lower voltage than the other configurations. Thus, as also has been pointed out by previous authors^{14,36}, we find that first-principles calculations can provide predictions intercalation energies and hence, battery voltages.

An interesting aspect of the effect of cation ordering on average voltage is that LiCoO_2 in the V2 structure has a much higher average voltage than CuPt. This increase in voltage is of interest because V2 is a $(\text{LiO})_2(\text{CoO})_2$ (111) superlattice, whereas CuPt is a $(\text{LiO})_1(\text{CoO})_1$ (111) superlattice. If one exchanges every other pair of cations in the CuPt layered sequence, the V2 layering is obtained. Thus, V2 is just CuPt with anti-sites on two out of every four layers. This suggests that anti-site defects Li_{Co} and Co_{Li} in the LiCoO_2 CuPt structure, while energetically very costly, should increase the voltage of the compound.

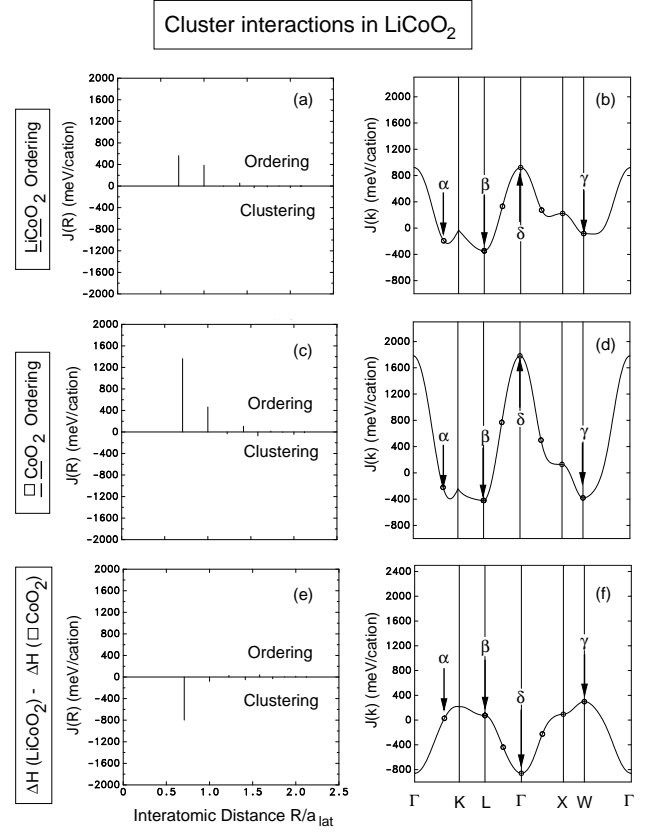


FIG. 4. Pair interaction energies J_f and $J(\mathbf{k})$ in both real (left) and reciprocal space (right). Interactions are shown for the cluster expansions of energies of Li/Co ordering in LiCoO_2 [(a) and (b)], energies of \square /Co ordering in $\square\text{CoO}_2$ [(c) and (d)], and average intercalation voltage in LiCoO_2 [(e) and (f)]. In real space, positive values of J_f indicate a preferred tendency for unlike atoms (“ordering”) and negative values indicate a tendency for like atoms (“clustering”). The labels α , β , γ , and δ indicate the $\frac{1}{2}[110]$, $\frac{1}{2}[111]$, $\frac{1}{2}[201]$, and $[000]$ points in reciprocal space, which correspond to the ordering waves of the Y2, (CuPt and D4), CH, and phase separated structures, respectively.

IV. CLUSTER EXPANSIONS OF Li/Co AND \square /Co ORDERING AND ΔH_{react}

We can now use the set of first-principles calculated energetics described in Section III to determine a set of interaction coefficients of the cluster expansion [Eq. (1)] for cation ordering. We have constructed three cluster expansions of three different types of ordering: (i) Li/Co ordering in LiCoO_2 , (ii) \square /Co ordering in $\square\text{CoO}_2$, and (iii) cation ordering effects on the average intercalation voltage (see below).

The pair interactions J_f found from our CE fits are shown in Fig. 4, both as real-space pairs $J(|\mathbf{R}_i - \mathbf{R}_j|)$ and as the lattice Fourier transform in reciprocal space $J(\mathbf{k})$. We see that the pair interactions in real space are decaying with distance quite quickly, indicating con-

vergence of the expansion. In reciprocal space, the pair interactions in Fig. 4 show some interesting properties: Minima in $J(\mathbf{k})$ indicate wavevectors where composition waves are likely to form low energy structures. The four body interactions J_4 found from our CE fits are much smaller than the pair interactions (e.g., J_2) with the ratio $J_4/J_2=0.004, 0.02,$ and 0.04 for the types of ordering (i)-(iii) above.

For Li/Co ordering in LiCoO_2 , the three *local* minima of $J(\mathbf{k})$ are located at three wavevectors (shown by bold arrows in Fig. 4): L-point $\frac{1}{2}(111)$, W-point $\frac{1}{2}(201)$, and near the K-point $\frac{1}{2}(110)$. (Additionally, an extremely shallow minima occurs between the Γ and X points.) These three wavevectors are the composition waves used to build all of the structures in the LiMO_2 series: CuPt and D4 [$\frac{1}{2}(111)$], CH [$\frac{1}{2}(201)$], and Y2 [$\frac{1}{2}(110)$]. The *global* minimum of $J(\mathbf{k})$ occurs at the L-point [$\frac{1}{2}(111)$], the composition wave used to construct the CuPt and D4 structures. Thus, we anticipate that the pair interactions $J(\mathbf{k})$ for cation ordering in other LiMO_2 systems (for other transition metals M) is likely to be qualitatively similar to that of Fig. 4 with changes in the relative minima at these three points. For \square/Co ordering in $\square\text{CoO}_2$, the minima in $J(\mathbf{k})$ occur at the same points as in the case of Li/Co ordering in LiCoO_2 , indicating that the relative ordering tendencies are similar in the two systems.

For the cluster expansion of average intercalation energy, the minimum of $J(\mathbf{k})$ occurs at the Γ point, the origin of reciprocal space (also shown by a bold arrow in Fig. 4, δ), indicating that phase separation into $\text{LiO}+\text{CoO}$ should produce a low ΔH_{react} , and hence a high voltage.

Once the interactions $\{J_f\}$ are obtained, Eq. (1) provides an efficient parameterization of the energy of *any* configuration. Applications of this cluster expansion parameterization which we now discuss include a search of configuration space (via a Monte Carlo simulated annealing algorithm) for ground state structures, which need not necessarily be included in the input set, thus opening the possibility of discovering unsuspected low energy states. One can also perform Monte Carlo simulations at finite temperatures to assess the thermodynamic and order-disorder properties of the system. Finally, one can easily calculate the energetics of disordered and partially ordered cation arrangements in these systems.

As pointed out previously, the cluster expansions use as input only charge compensated compounds, and therefore can be used to predict the energies of charge compensated $(\text{LiO})^* + (\text{CoO})^*$. We find from our CE of LiCoO_2 that $(\text{LiO})^* + (\text{CoO})^*$ is 0.79 eV/formula unit lower in energy than the nominal, non-charge-compensated $\text{LiO}+\text{CoO}$. Similarly, the CE of $\square\text{CoO}_2$ predicts that $(\square\text{O})^* + (\text{CoO})^*$ is 0.84 eV below the non-compensated compounds.

A. Ground States

The simulated annealing algorithm finds the CuPt structure as the low temperature state. In Table III, we simply note that this structure was the lowest in energy of the eight structures calculated by LAPW. But, the simulated annealing prediction of the ground state demonstrates that CuPt is also the lowest energy configuration out of an astronomical number of possible configurations (without symmetry, there are $\sim 2^N$ possible configurations that the algorithm could explore, where $N=4096$). For our cluster expansion of $\square\text{CoO}_2$, the simulated annealing algorithm also finds CuPt as the lowest energy substitutional configuration. As we have already shown above, non-substitutional configurations are even lower in energy for the $\square\text{CoO}_2$ system (e.g., the CdI_2 structure).

By combining the simulated annealing algorithm with the cluster expansion of average voltage, one can search for the cation configuration with *maximum* voltage. This search yields a phase separated ($\text{LiO}+\text{CoO}$) configuration (5.8 V). De-intercalating Li from this configuration would correspond to the artificial case of: $\text{LiO} \rightarrow \text{Li} + \square\text{O}(\text{fcc})$. It is interesting to note that other authors³⁶ by very different means have also arrived at the conclusion that this admittedly artificial case corresponds to the theoretical maximum voltage in LiMO_2 compounds.

B. Order-Disorder Transitions

For LiCoO_2 , the order-disorder transition between the low-temperature CuPt phase and the high-temperature disordered phase is predicted to occur at ~ 5100 K (Fig. 5), well above the melting point of this material. (Note that the calculations in this paper are all solid-state, and thus do not consider the liquid phase.) Antaya *et al.*³⁴ report a disordered rocksalt phase of LiCoO_2 , grown by laser ablation deposition at 150°C , whereas growth at higher temperatures results in either the D4 or CuPt phases. Our calculations indicate that the observed³⁴ disordered rocksalt phase of LiCoO_2 is *not thermodynamically stable*, but is rather only stabilized kinetically, consistent with the fact that the disordered phase can only be grown at low temperatures. By performing a simulation of \square/Co ordering $\square\text{CoO}_2$ at finite temperatures, we were able to ascertain the effect of vacancies on the order-disorder transition temperature. Upon complete removal of Li, the order-disorder transition of $\square\text{CoO}_2$ drops to ~ 4400 K, still much too high to be experimentally accessible. Thus, the addition of Li vacancies is not likely to make the disordered rocksalt phase thermodynamically accessible to experiments (although this phase is still kinetically accessible).

At temperatures below 2000 K, the CuPt structure is predicted to be completely ordered. Thus, at any growth temperatures where thermodynamic equilibrium

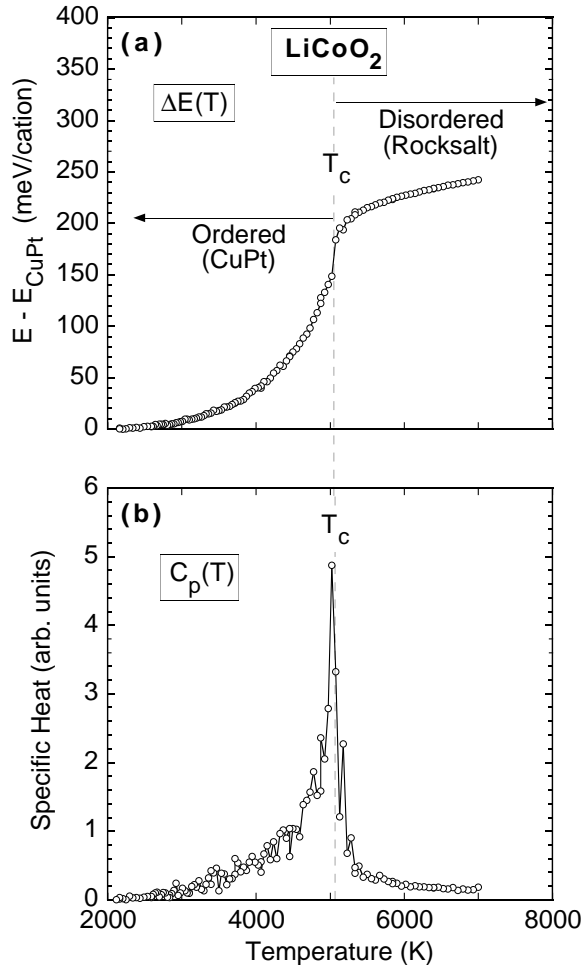


FIG. 5. Monte Carlo calculated (a) energy relative to the $T=0$ energy of the CuPt structure and (b) heat capacity as functions of temperature for LiCoO_2 . The transition between the CuPt and disordered (rocksalt) LiCoO_2 can be seen at ~ 5100 K.

is achieved, the CuPt phase should form with a long-range order (LRO) parameter of nearly unity. Thus, anti-site defects Li_{Co} or Co_{Li} are probably not formed under conditions of thermodynamic equilibrium. Also, since CuPt is completely ordered by 2000K, even the D4 structure is not stabilized by thermodynamic factors (i.e., thermal fluctuations in energy are smaller than the CuPt-D4 energy difference for temperatures of interest). However, the D4 structure has been observed in low-temperature solution grown and laser ablation-grown samples, which are probably not equilibrium phases.

C. Properties of Disordered and Partially Ordered Cation Arrangements

Using the CE, we can compute the energetics of *any* cation arrangement such as random alloys or any disordered (short-range or long-range ordered) phases. These

are examples of phases which are not directly accessible to first-principles calculations, but may be accessed via the cluster expansion. We show the cluster expansion energetics of several such phases in Table III:

Random alloy: The perfectly random alloy is a phase in which Li and Co atoms (or \square and Co for $\square\text{CoO}_2$) are distributed on their cation fcc sublattice with no atom-atom correlation between cation sites. This corresponds to the enthalpy as $T \rightarrow \infty$. The energy of this random phase is easily computed from the cluster expansion of Eq. (1), since the absence of atomic correlations leads to the simple values $\bar{\Pi}_f = 0$, and thus the energy of the random alloy is given by $E_{\text{CE}}(\text{Random}) = J_0$. The energies of random cation arrangements in LiCoO_2 and $\square\text{CoO}_2$ are shown in Table III. The ordering energy of an ordered compound σ is the energy required to construct σ from the random cation arrangement: $\delta E_{\text{ord}}(\sigma) = E(\sigma) - E(\text{Random})$. From Table III, we can see that for both LiCoO_2 and $\square\text{CoO}_2$, all ordered cation configurations considered have $\delta E_{\text{ord}} < 0$, except for CA, V2, and Z2.

Partial Short-Range Order: Because Antaya *et al.*³⁴ report the existence of some degree of CuPt-type ordering in their disordered phase, we have also computed (Table III) the energetics of a disordered rocksalt phase with some degree of atomic short-range order (SRO). SRO is a finite-temperature effect, and is characterized in real space by the pair correlation functions $\bar{\Pi}_{0,n} \neq 0$ for the n th atomic shell. Thus, the SRO parameters, $\bar{\Pi}_{0,n}$ measure the extent to which spatial correlations exist in disordered alloys. The SRO parameters used to compute the energetics of for the first ten neighbor shells were obtained from a Monte Carlo simulation of the LiCoO_2 disordered alloy just above the order-disorder transition (in parentheses are the values for fully ordered CuPt or D4): $-0.06(0.0)$, $-0.27(-1.0)$, $+0.03(0.0)$, $+0.12(+1.0)$, $+0.02(0.0)$, $-0.07(-1.0)$, $-0.02(0.0)$, $+0.10(1.0)$, $-0.01(0.0)$, and $-0.01(0.0)$. Note that the energetic effect of SRO is to significantly lower the energy of the random phase in both LiCoO_2 and $\square\text{CoO}_2$ by 0.27 and 0.40 eV/formula unit, respectively.

Partial Long-Range Order: There have also been reports of long-range ordered LiCoO_2 (either CuPt or D4) with small quantities of Li on the Co sites, or vice versa. This amounts to a CuPt or D4 phase with partial long-range order (LRO). If the LRO parameter $\eta=1$, then all Li and Co atoms reside completely on their own sublattice and LRO is perfect. However, for states of partial LRO, $\eta < 1$, and there is an amount $\frac{1-\eta}{2}$ of intermixing between sublattices. For simplicity, we assume that there are no short-range correlations between the intermixed atoms. In Table III, we show the energetics of CuPt and D4 structures with LRO parameter $\eta=0.88$, corresponding to 6% of Li on the Co sites, and vice versa. The LiCoO_2 energies of CuPt and D4 are both raised by 0.16 eV/formula unit relative to the $\eta=1$ fully ordered phases, while the corresponding increases for $\square\text{CoO}_2$ is 0.20 and

0.17 eV/formula unit.

The cluster expansion of voltage can also be used to predict the average voltages of configurations not directly accessible to first-principles calculations (Table III). In particular, we see that the random alloy (3.99 V) is predicted to have a higher average voltage than the ordered CuPt phase (3.78 V). Since this phase has been produced by laser ablation,³⁴ it would be interesting to measure its electrochemical properties, in order to compare with our predictions. The increase in voltage due to disorder is significantly reduced when one considers the disordered phase with SRO described above (3.86 V). Thus, it is possible that experimentally, the voltage of the disordered LiCoO₂ relative to CuPt could be used to indirectly determine the amount of short-range order in the sample. Also in Table III are the voltages of partially long-range ordered CuPt and D4 phases with 6% of the Co atoms on the Li sites ($\eta=0.88$). Even this small amount of anti-site defects increases the voltages of CuPt and D4 by 0.05 and 0.01 V, respectively. Note that for either LRO or SRO, the qualitative effect of disordering is the same: Disorder raises the energy of $\square\text{CoO}_2$ more than LiCoO₂, and thus raises the average voltage.

V. ENERGETICS OF OCTAHEDRAL VS. TETRAHEDRAL ABC_2 NETWORKS

We now compare our results for cation ordering in the octahedral LiCoO₂ and $\square\text{CoO}_2$ systems with the well-studied cases of cation ordering in isovalent and heterovalent tetrahedral ABC_2 systems. In the (heterovalent) octahedral LiMO₂ systems, ordered cation arrangements are *stable* with respect to LiO+MO. This ordered compound stability is qualitatively similar to heterovalent tetrahedral systems, such as CuInSe₂, where cation ordered phases are stable relative to decomposition into CuSe+InSe zincblende binaries. Just as in the LiCoO₂ case, the binaries correspond to compounds (rocksalt LiO and CoO and zincblende CuSe and InSe) which do not satisfy the octet rule, and hence are relatively high energy configurations. The high energy of the constituents “exposes” the ordered compounds (which do satisfy the octet rule) as stable in these I-III-VI₂ systems. The stability of ordered compounds in octahedral LiMO₂ systems is, however, in contrast to the isovalent tetrahedral $A^{III}B^{III}C_2^V$ systems, in which bulk ordered compounds are unstable with respect to AC+BC. In these III-III-V₂ systems, the phase-separated state is the low energy ground state, and ordered compounds which have been observed have been shown¹ to be a result of a combination of epitaxial strain and surface-reconstruction-induced ordering.

The relative order of energies of ordered compounds in the octahedral LiCoO₂ and $\square\text{CoO}_2$ systems is also quite different from the (isovalent or heterovalent) tetrahedral cases: $E(\text{CuPt}) < E(\text{CH}) < E(\text{CA})$ in both LiCoO₂ and

$\square\text{CoO}_2$, compared with $E(\text{CH}) < E(\text{CA}) < E(\text{CuPt})$, universally found in the lattice-mismatched tetrahedral systems. Also, in the octahedral systems, the ordering energy $\delta E_{\text{ord}} < 0$ for both CuPt and CH, while $\delta E_{\text{ord}} < 0$ for CH in the tetrahedral systems.

The CuPt structure is preferred in octahedral networks due to strain energy arguments: For an octahedral ABC_2 system which has distinct equilibrium $A-C$ and $B-C$ bond lengths, the CuPt structure has the property that the cell-internal distortion of the anions (C) accommodates *any* equilibrium $A-C$ and $B-C$ bond lengths, and maintains all $A-C$ bond lengths equal to one another (and similarly for $B-C$). The D4 structure also possesses this optimal structural relaxation. This optimal bond-length accommodation is interesting in light of the fact that the cation CuPt structure in *tetrahedral* systems, when relaxed, possesses two equilibrium $A-C$ bonds (and similarly for $B-C$) as opposed to the single $A-C$ bond in the octahedral case. The distinction between the two $A-C$ bonds in *tetrahedral* CuPt is due to the fact that some of the $A-C$ bonds in this structure are along the direction of cell-internal distortion and other $A-C$ bonds are perpendicular to this direction. Thus, when C atoms are relaxed, these two types of $A-C$ bonds adopt different bond lengths. However, in the *octahedral* CuPt structure, none of the $A-C$ bonds are either along or perpendicular to the distortion direction of the anions, but rather all $A-C$ bonds are at equivalent angles to this direction. Thus, when the anions relax, all $A-C$ bonds are distorted by equal amounts. The calculated equilibrium bond lengths in all cation arrangements for LiCoO₂ are given in Table IV. One can see from this table that CuPt and D4 are the only structures for which there is only one type of symmetry-inequivalent Li-O and Co-O bond. Structures with Li-O and Co-O bonds equal to one another (e.g., CH, CA) are energetically unfavorable. In tetrahedral systems, the configuration which possess the optimum structural geometry, analogous to CuPt in octahedral coordination, is the CH structure, which is the lowest energy ordered compound in size mismatched semiconductor alloys. This strain energy argument can also explain the relative stability of CuPt, CH, and CA in octahedral *vs.* tetrahedral systems: Using a simple valence force field which includes only energetic effects due to strain, one obtains the correct order of these three structures for both octahedral and tetrahedral systems as compared with LAPW.^{37,38,39} One should note, however, that in the LiMO₂ series, there are systems other than $M=\text{Co}$ which possess ground states other than CuPt, e.g., the CH and Y2 structures. Thus, clearly strain-only arguments do not explain the totality of ordering tendencies in these compounds, as other effects must dominate in some systems.

Another distinction between the ordering tendencies of the octahedral LiCoO₂ system with those of the tetrahedral systems is in the energy scale. In Fig. 2, the energy scale of the tetrahedral systems is multiplied by a factor of 5, and is still smaller than the octahedral energy scale.

TABLE IV. Calculated bonds lengths in various cation arrangements of LiCoO₂.

Cation Structure	Li-O (Å)	Co-O (Å)
CuPt	2.08	1.90
D4	2.05	1.91
Y2	1.93,2.08,2.28	1.86,1.92,1.94
CH	1.94,2.24	1.89,1.94
W2	1.93,1.97,2.09,2.12	1.86,1.90,1.93,1.98
CuAu	1.87,1.99	1.87,1.99
V2	1.89,2.21	1.84,2.04
Z2	1.99,2.04,2.35	1.76,1.96,1.99

The difference between the energy of the highest and lowest ordered compounds in the isovalent tetrahedral III-III-V₂ systems is $\delta E(\text{CuPt-CH}) \sim 0.1$ eV/formula unit, in the heterovalent tetrahedral CuInSe₂ system it is $\delta E(\text{V2-CH}) \sim 0.7$ eV/formula unit, whereas this difference in the octahedral systems is $\delta E(\text{V2-CuPt}) \sim 1.4$ eV/formula unit in the LiCoO₂ system and $\delta E(\text{V2-CuPt}) \sim 2.4$ eV/formula unit in $\square\text{CoO}_2$. Thus the energetic effect of cation ordering is much more dramatic in the octahedrally coordinated networks.

VI. SUMMARY

Using a combination of first-principles total energy calculations, a cluster expansion approach, and Monte Carlo simulated annealing, we have studied the cation ordering in LiCoO₂ and $\square\text{CoO}_2$, and compared the ordering in these heterovalent octahedrally coordinated systems with previous studies of ordering in both isovalent and heterovalent tetrahedral ABC_2 systems. We find many significant differences between ordering in octahedral and tetrahedral systems. In the heterovalent octahedral systems, ordered compounds have negative formation energies, and are hence *stable*. This is qualitatively similar to the heterovalent tetrahedral case, but distinct from the isovalent tetrahedral semiconductors, where ordered cation arrangements are unstable. Also, the relative order of ordered compound energies is different in the octahedral systems studied here, relative to either isovalent or heterovalent tetrahedral systems. In particular, for both the LiCoO₂ and $\square\text{CoO}_2$ systems, a simulated annealing ground state search of the entire cation configuration space yields the CuPt cation arrangement as the lowest energy ground state, whereas this structure is the *highest* energy configuration in tetrahedral III-III-V₂ systems. The scale of ordering energetics is dramatically different in the LiCoO₂ and $\square\text{CoO}_2$ octahedral systems (~ 1.5 - 2.5 eV), compared with that of either heterovalent (e.g., ~ 0.7 eV in CuInSe₂) or isovalent tetrahedral semiconductors (~ 0.1 eV). This difference in energy scales is also reflected in the different temperature scales of order-disorder problems in the two types of systems: While typical order-disorder temperatures in isovalent or heterovalent tetrahedral systems are $\lesssim 1000$ K, we find tran-

sition temperatures of ~ 5100 K and ~ 4400 K for LiCoO₂ and $\square\text{CoO}_2$, respectively.

Because LiCoO₂ is in a class of materials being studied for use in rechargeable Li batteries, we have also examined the effects of cation ordering on Li intercalation energies and average voltages in Li_xCoO₂/Li cells. Searching the space of configurations σ for large average voltages, we find that $\sigma = \text{CuPt}$ [a monolayer $\langle 111 \rangle$ superlattice] has a high voltage ($\bar{V} = 3.78$ V), but that this could be increased by cation randomization ($\bar{V} = 3.99$ V), partial disordering ($\bar{V} = 3.86$ V), or by forming a 2-layer Li₂Co₂O₄ superlattice along $\langle 111 \rangle$ ($\bar{V} = 4.90$ V).

Acknowledgements

The authors gratefully acknowledge many helpful discussions with Su-Huai Wei about the LAPW method and ordering in semiconductor systems, and with Melissa Fu, David Ginley, Jeanne McGraw, Phil Parilla, John Perkins, and Doug Trickett about the experimental aspects of this problem. Work at NREL was supported by the Office of Energy Research (OER) [Division of Materials Science of the Office of Basic Energy Sciences (BES)], U. S. Department of Energy, under contract No. DE-AC36-83CH10093.

-
- ¹ A. Zunger and S. Mahajan, in *Handbook on Semiconductors*, Vol. 3, Elsevier (1993).
 - ² T. A. Hewston and B. L. Chamberland, *J. Phys. Chem. Solids* **48**, 97 (1987).
 - ³ W. Li, J. N. Reimers, and J. R. Dahn, *Phys. Rev. B* **49**, 826 (1994).
 - ⁴ S. -H. Wei and A. Zunger, *Phys. Rev. B* **48**, 6111 (1993); **55**, 13605 (1997).
 - ⁵ K. Mizushima, P. C. Jones, P. J. Wiseman, and J. B. Goodenough, *Mat. Res. Bull.* **15**, 783 (1980).
 - ⁶ *Solid State Batteries: Materials Design and Optimization*, C. Julien and G. -A. Nazri, eds. Kluwer, Boston (1994), Chap. 1.
 - ⁷ R. J. Gummow and M. M. Thackeray, *Solid State Ionics* **53**, 681 (1992).

- ⁸ R. J. Gummow, D. C. Liles, M. M. Thackeray, and W. I. F. David, *Mat. Res. Bull.* **28**, 1177 (1993).
- ⁹ E. Rossen, J. N. Reimers, and J. R. Dahn, *Solid State Ionics* **62**, 53 (1993).
- ¹⁰ M. Antaya, J. R. Dahn, J. S. Preston, E. Rossen, and J. N. Reimers, *J. Electrochem. Soc.* **140**, 575 (1993).
- ¹¹ G. G. Amatucci, J. M. Tarascon, and L. C. Klein, *J. Electrochem. Soc.* **143**, 1114 (1996).
- ¹² J. N. Reimers and J. R. Dahn, *J. Electrochem. Soc.* **139**, 2091 (1992).
- ¹³ T. Ohzuku, A. Ueda, M. Nagayama, Y. Iwakoshi, and H. Komori, *Electrochimica Acta* **38**, 1159 (1993).
- ¹⁴ J. N. Reimers and J. R. Dahn, *Phys. Rev. B* **47**, 2995 (1993).
- ¹⁵ D. J. Singh, *Planewaves, Pseudopotentials, and the LAPW Method*, (Kluwer, Boston, 1994).
- ¹⁶ S.-H. Wei and H. Krakauer, *Phys. Rev. Lett.* **55**, 1200 (1985) and references therein.
- ¹⁷ D. de Fontaine, *Solid State Physics* **34**, 73 (1979).
- ¹⁸ J. Kanamori and Y. Kakehashi, *J. Phys. (Paris) Colloq.* **38**, C7-274 (1977).
- ¹⁹ J. M. Sanchez, F. Ducastelle, and D. Gratias, *Physica A* **128**, 334 (1984).
- ²⁰ F. Ducastelle, *Order and Phase Stability in Alloys*, Elsevier, New York (1991).
- ²¹ D. de Fontaine, *Solid State Physics* **47**, 33 (1994).
- ²² A. Zunger, in *Statics and Dynamics of Alloy Phase Transformations*, edited by P. E. A. Turchi and A. Gonis, NATO ASI Series (Plenum, New York, 1994).
- ²³ K. Binder, *Monte Carlo Methods in Statistical Physics: An Introduction*, Springer-Verlag, New York (1992); *Applications of the Monte Carlo Method in Statistical Physics*, edited by K. Binder, Springer-Verlag, New York (1987).
- ²⁴ S.-H. Wei, L. G. Ferreira, and A. Zunger, *Phys. Rev. B* **45**, 2533 (1992).
- ²⁵ G. Ceder, *Comp. Mater. Sci.* **1**, 144 (1993).
- ²⁶ Z. -W. Lu, S. -H. Wei, A. Zunger, S. Frota-Pessoa, and L. G. Ferreira, *Phys. Rev. B* **44**, 512 (1991).
- ²⁷ For CuPt in the ideal geometry (with all atoms in ideal rocksalt positions), $c/a = 2\sqrt{6}=4.899$, whereas the observed $(4.98)^{13}$ and calculated values (4.84) differ from this ratio (Table II).
- ²⁸ L.G. Ferreira, S.-H. Wei, and A. Zunger, *Int. J. of Supercomputer Applications* **5**, 34-56 (1991).
- ²⁹ D. B. Laks, L. G. Ferreira, S. Froyen, and A. Zunger, *Phys. Rev. B* **46**, 12587 (1992).
- ³⁰ D. M. Ceperley and B. J. Alder, *Phys. Rev. Lett.* **45**, 566 (1980); J. P. Perdew and A. Zunger *Phys. Rev. B* **23**, 5048 (1981).
- ³¹ S. Froyen, *Phys. Rev. B* **39**, 3168 (1989); H. J. Monkhorst and J. D. Pack, *Phys. Rev. B* **13**, 5188 (1976).
- ³² It is well known that CoO is a Mott insulator, and the local density approximation incorrectly predicts that the compound is a metal. However, in considering cation ordering, LiO+CoO is simply a constant reference point for these calculations, and so errors in the LDA CoO energy will shift all formation energies of LiCoO₂ and □CoO₂ by a constant amount, and hence will not affect any of our statements about ordering in LiCoO₂ or □CoO₂.
- ³³ R. J. Gummow, D. C. Liles, and M. M. Thackeray, *Mat. Res. Bull.* **28**, 235 (1993).
- ³⁴ M. Antaya, K. Cearnis, J. S. Preston, J. N. Reimers, and J. R. Dahn *J. Appl. Phys.* **76**, 2799 (1994).
- ³⁵ B. Garcia, P. Barvoux, F. Ribot, A. Kahn-Harari, L. Mazerolles, and N. Baffier, *Solid State Ionics* **80**, 111 (1995).
- ³⁶ M. K. Aydinol, A. F. Kohan, G. Ceder, K. Cho, and J. Joannopoulos, *Phys. Rev. B* **56**, 1354 (1997).
- ³⁷ L. Bellaiche (private communication).
- ³⁸ A. Silverman, A. Zunger, R. Kalish, and J. Adler, *Phys. Rev. B* **51**, 10795 (1995).
- ³⁹ S.-H. Wei, L. G. Ferreira, and A. Zunger, *Phys. Rev. B* **41**, 8240 (1990).
- ⁴⁰ M. Antaya, J. R. Dahn, J. S. Preston, E. Rossen, and J. N. Reimers, *J. Electrochem. Soc.* **140**, 575 (1993).